# Cell Wall Architecture of the Elongating Maize Coleoptile[1]

**Nicholas C. Carpita, Marianne Defernez, Kim Findlay, Brian Wells, Douglas A. Shoue, Gareth Catchpole, Reginald H. Wilson, and Maureen C. McCann***

Department of Botany and Plant Pathology, Purdue University, West Lafayette, Indiana 47907–1155 (N.C.C., D.A.S.); Department of Food Metrology, Institute of Food Research, Norwich Research Park, Colney, Norwich NR4 7UA, United Kingdom (M.D., G.C., R.H.W.); and Department of Cell and Developmental Biology, John Innes Centre, Norwich Research Park, Colney, Norwich NR4 7UH, United Kingdom (K.F., B.W., M.C.M.)

The primary walls of grasses are composed of cellulose microfibrils, glucuronoarabinoxylans (GAXs), and mixed-linkage β-glucans, together with smaller amounts of xyloglucans, glucomannans, pectins, and a network of polyphenolic substances. Chemical imaging by Fourier transform infrared microspectroscopy revealed large differences in the distributions of many chemical species between different tissues of the maize (*Zea mays*) coleoptile. This was confirmed by chemical analyses of isolated outer epidermal tissues compared with mesophyll-enriched preparations. Glucomannans and esterified uronic acids were more abundant in the epidermis, whereas β-glucans were more abundant in the mesophyll cells. The localization of β-glucan was confirmed by immunocytochemistry in the electron microscope and quantitative biochemical assays. We used field emission scanning electron microscopy, infrared microspectroscopy, and biochemical characterization of sequentially extracted polymers to further characterize the cell wall architecture of the epidermis. Oxidation of the phenolic network followed by dilute NaOH extraction widened the pores of the wall substantially and permitted observation by scanning electron microscopy of up to six distinct microfibrillar lamellae. Sequential chemical extraction of specific polysaccharides together with enzymic digestion of β-glucans allowed us to distinguish two distinct domains in the grass primary wall. First, a β-glucan-enriched domain, coextensive with GAXs of low degrees of arabinosyl substitution and glucomannans, is tightly associated around microfibrils. Second, a GAX that is more highly substituted with arabinosyl residues and additional glucomannan provides an interstitial domain that interconnects the β-glucan-coated microfibrils. Implications for current models that attempt to explain the biochemical and biophysical mechanism of wall loosening during cell growth are discussed.

Biochemical studies have provided a reasonably complete catalog of the major polysaccharides and phenolic substances that constitute the primary cell walls of angiosperms (McCann and Roberts, 1991; Carpita and Gibeaut, 1993). The walls of grasses and related monocots (commelinoids) have quite different compositions compared with those of all dicots and of the non-commelinoid monocot species (Carpita, 1996). The "type II" cell walls of commelinoid monocots are characterized by cellulose microfibrils cross-linked by glucuronoarabinoxylans (GAXs) and a network of polyphenolic substances (Carpita and Gibeaut, 1993; Carpita, 1996). Maize (*Zea mays*) and other members of the Poales also contain developmentally regulated polymers, the mixed-linkage (1→3),(1→4)-β-D-glucans (hereafter, called β-glucans). The β-glucans are initially absent from meristematic cells but accumulate up to about 20% dry mass of the cell wall coincident with the most rapid rates of coleoptile elongation (Kim et al., 2000). As the elongation rate slows, the β-glucan is hydrolyzed by exo- and endo-β-D-glucanases located in the wall. Concomitant with the decrease in β-glucan, there is an increase in the content of etherified and esterified hydroxycinnamic acids and other related lignin-like aromatic substances associated with the cessation of growth (Carpita, 1986; Müsel et al., 1997). The coleoptile is a convenient model to examine the dynamic changes in cellular architecture during cell elongation in grasses; the polymer composition and architectural changes that occur in this organ reflect those of the primary wall of all developing cells (for review, see Carpita, 1996). The β-glucans are present in all mature cereal tissues in low amounts, perhaps a consequence of similar mechanisms of hydrolysis after cell expansion has stopped.

Despite an extensive knowledge of the chemical structure of the wall polymers of grasses, the interactions of these molecules when assembled into a cell wall architecture have largely been deduced on the basis of their extractability from bulk samples. Fourier transform infrared (FTIR) spectroscopy uses infrared (IR) light to probe carbohydrate and phenolic molecules without derivatization of the sample (Mc-

[1] This work was supported by the U.S. Department of Energy, Energy Biosciences (grant to N.C.C.), by the Biotechnology and Biological Sciences Research Council (grant to R.H.W. and M.C.M.), and by a Royal Society University Research Fellowship (to M.C.M.). This is journal paper no. 16,541 of the Purdue University Agriculture Experiment Station.

* Corresponding author; e-mail maureen.mccann@bbsrc.ac.uk; fax 44–1603–450–022.

Article, publication date, and citation information can be found at www.plantphysiol.org/cgi/doi/10.1104/pp.010146.

Cann et al., 1992, 1997; Séné et al., 1994). By use of a microscope attachment, the localization of molecules in individual cells may be deduced by using double-bladed apertures to mask off an area of tissue section from which spectral data is to be collected (McCann et al., 1997; Himmelsbach et al., 1999). The synergy of what have traditionally been two distinct methods for studying the chemistry and morphology of a sample, IR spectroscopy and optical microscopy, has been called chemical imaging (McCann et al., 1997; Himmelsbach et al., 1999). In chemical imaging, the sample, mounted on the stage of an IR microscope, is moved under computer control such that different areas of the sample are measured sequentially. These spectral arrays can be correlated with visual images of the sample so that optically observed features can be associated with functional groups. Contrast in IR spectroscopic imaging is determined by differences in the absorbance of specific frequencies, using color to represent relative absorbance intensities.

In this paper, we have used chemical imaging to reveal the intrinsic heterogeneity in different tissues of the maize coleoptile. We have isolated the mesophyll and epidermal cells of the coleoptile from each other, and determined their polymer compositions by sugar and linkage analyses. Using a monoclonal antibody as a specific probe for β-glucans, we have confirmed the relative abundance of this molecule in mesophyll cell walls. This localization has implications for models in which the β-glucans become load bearing during cell elongation. During growth, the outer epidermis is thought to be the major load-bearing structure of the organ (Kutschera, 1989). The walls of the outer epidermis can be isolated relatively easily, and so we have applied field emission scanning electron microscopy (FESEM) and IR spectroscopy to examine the architecture of this tissue. We have sequentially extracted polymers from walls of epidermal peels and characterized them chemically. We imaged the residual wall material by FESEM, and obtained IR spectra of this material. These data allow us to propose a modified model of architecture for the type II primary cell walls of the maize coleoptile.

**Table I.** *Comparison of the linkage structure of neutral cell wall polysaccharides from epidermis and mesophyll cells of the elongating maize coleoptile*

Linkage refers to the hydroxyl position upon which another sugar is attached and is inferred from methylation analysis. For example, 4-Glc is itself attached to another sugar via its anomeric carbon (C-1), which is understood, and another sugar was attached at its O-4 position. The actual derivative is 2,3,6-tri-*O*-methyl-(1-deuterio)-1,4,5-tri-*O*-acetylglucitol. *t*-Glc is a nonreducing end-terminal glucosyl residue. tr, Trace.

| Sugar and Linkage | Epidermis | Mesophyll |
|---|---|---|
| | *mol %* | |
| Fuc | | |
| *t*-Fuc | 0.6 | 0.3 |
| Rhamnose | | |
| 2-Rha | 0.8 | 0.9 |
| 2,4-Rha | 1.9 | 1.0 |
| Ara | | |
| *t*-Ara | 25.9 | 21.2 |
| 2-Ara | 0.1 | 0.1 |
| 3-Ara | 1.1 | 0.8 |
| 5-Ara | 1.7 | 1.5 |
| 3,5-Ara | 0.4 | 0.3 |
| Xyl | | |
| *t*-Xyl | 3.2 | 4.9 |
| 2-Xyl | 1.1 | 1.2 |
| 4-Xyl | 4.4 | 4.5 |
| 3,4-Xyl | 27.7 | 20.6 |
| Man | | |
| *t*-Man | tr | tr |
| 4-Man | 2.6 | 1.2 |
| 4,6-Man | 0.4 | 0.2 |
| Gal | | |
| *t*-Gal | 3.9 | 3.3 |
| 3-Gal | tr | 0.6 |
| 4-Gal | 1.4 | 2.8 |
| 6-Gal | 0.5 | 0.8 |
| 3,6-Gal | 1.1 | 0.2 |
| Glc | | |
| *t*-Glc | 0.1 | 0.2 |
| 3-Glc | 3.1 | 4.8 |
| 4-Glc | 14.9 | 23.9 |
| 4,6-Glc | 2.4 | 3.4 |

## RESULTS

### Quantitation of Cell Wall Polysaccharides in Mesophyll and Epidermal Tissues of Maize Coleoptiles

Cell walls from isolated epidermal or mesophyll cells were prepared. Three-day-old maize coleoptiles about 3.5 cm long were harvested and epidermal layers removed by peeling. Cell walls were prepared from the resulting mesophyll-enriched material and from the epidermal peels, and analyzed for cellulose content, uronic acid and ester content, sugar composition, and linkage analysis (Tables I and II). The cell walls of epidermis and mesophyll cells are distinct chemically. Whereas cellulose (measured as material resistant to acetic-nitric digestion; Updegraff, 1969) constitutes about 30% of the mesophyll wall mass, the thick epidermal wall comprises almost 60% cellulose (Table II). Although similar polymers constitute the walls of mesophyll and epidermis, the relative proportions of these polymers are different. Both cell types have substantial amounts of β-glucan, as judged both by the appearance of 3-linked glucan in the methylation analysis and by direct measurement by digestion with a *Bacillus subtilis* (1→3),(1→4) β-D-glucan endo-4-glucanohydrolase (β-glucan endohydrolase) and quantitation of the diagnostic oligomers by high-performance anion-exchange chromatography (HPAEC)-pulsed-amperometric detection. The epidermis contains about 60 μg of β-glucan per mg cell wall, whereas the mesophyll cells contain almost 200 μg of β-glucan per mg cell wall (Table II). In contrast, the epidermis contains a higher proportion

**Table II.** *Estimation of polysaccharide contributions per total cell wall mass*

| Component | Epidermis | Mesophyll |
|---|---|---|
| | *μg mg cell wall*$^{-1}$ | |
| Cellulose | 594 | 284 |
| Cross-linking glycans | | |
| GAX | 195 | 312 |
| β-Glucan | 58 | 197 |
| Xyloglucan | 23 | 67 |
| Glucomannan | 19 | 12 |
| Arabinan | 13 | 26 |
| Pectic substances | | |
| GalA (homogalacturonan) | 71 | 56 |
| Rhamnogalacturonan I | 17 | 26 |
| Galactan and Arabinogalactan | 10 | 20 |

of glucomannan despite the much smaller total proportion of non-cellulosic polysaccharides (Table II). Despite differences in glucomannan content, the ratio of 4- and 4,6-linked mannosyl units is similar between mesophyll and epidermal walls. The vast majority of non-cellulosic polymers in both cell types are GAXs. The ratio of branched to unbranched xylosyl residues is significantly higher in the epidermal GAX (6.3:1) compared with mesophyll GAX (4.6:1; Table I). A small amount of xyloglucan is also present, based on the appearance of *t*-Xyl and 4,6-Glc. The small amount of galacturonic-acid-containing polymers has a degree of methyl esterification of 82% in walls from epidermal tissue compared with 75% in walls from mesophyll cells.

### Chemical Imaging of Sections of Maize Coleoptile

A 3-d-old maize coleoptile, an age at which elongation growth rate is highest, was sectioned transversely by hand, cleared of its soluble material, and mounted on a barium fluoride window for chemical imaging. Mapping software allowed the collection of 273 individual FTIR spectra with an aperture size of 25 × 25 μm in an array encompassing epidermal, vascular, and mesophyll cells from a transverse section of one-quarter of the coleoptile (Fig. 1A). The spectra in the data set were first baseline corrected and area normalized to compensate for any change in thickness across the section. To reveal the major spectral differences in the section, a principal component analysis (PCA) was applied to all spectra, and hence all tissue types. PCA is a mathematical operation that allows samples to be characterized by their scores on a small number of new variables (PC axes) instead of large numbers of original measurements (here, absorbances), thus summarizing the information and highlighting differences (Chen et al., 1998; Kemsley, 1998). Figure 1 (B–D) shows chemical images of the first 3 PC scores displayed as color intensities across the section. Contrast between tissues is particularly clear on PC2 and PC3 (accounting for, respectively, 30.8% and 6.7% of the variance in the data set). However, although there is a clear differentiation between the mesophyll and the inner epidermis with PC2, for the outer epidermis PC2 is only able to differentiate the epidermis close to the mesophyll: The very outer edge cannot be differentiated. Average spectra of mesophyll, and the inner and outer edges of the outer epidermis, shown in Figure 1 (middle), are different from each other. Inspection of the loadings for PC 2 and 3 allows us to determine that the origin of differentiation between the mesophyll and the epidermis generally, is related to the composition of these tissues, since the loadings exhibit features of carbohydrates. The second PC loading contains correlated peaks at 1,160, 1,105, 1,060, and 1,040 cm$^{-1}$, characteristic of cellulose (Tsuboi 1957; Liang and Marchessault, 1959), and perhaps also of β-glucan and glucomannan, two other polymers with (1→4) β-linked glucosyl units (see "Discussion"). The third PC loading has two major protein absorbances at 1,550 and 1,650 cm$^{-1}$ that may derive from cytoplasmic protein within the section, and negatively correlated methyl ester (1,740 and 1,245 cm$^{-1}$) and phenolic ester (1,720 cm$^{-1}$) peaks. Whereas Figure 1 gives an overview of how the relative peak intensities differ between tissues through the use of PCA, Figure 2 shows the absorbance of the material at particular frequencies of interest, displayed as chemical images. In each case, the peak height was ratioed to the area under the spectrum between 1,200 and 800 cm$^{-1}$ (the carbohydrate fingerprint region). Peaks corresponding to phenolic esters (1,720 cm$^{-1}$) or to methyl esters (1,740 cm$^{-1}$) were enriched in the vascular bundle, and slightly enhanced in the outer epidermis (Fig. 1, A and B). A peak corresponding to phenolic ring absorbance (1,515 cm$^{-1}$) is enriched in the vascular tissue, and is decreased in the inner epidermis (Fig. 1C). The chemical images thus indicate some differences between the inner and outer epidermis. Absorbances at 1,000 and 1,020 cm$^{-1}$ are enriched in the mesophyll layer (Fig. 1, D and E; selected from the loading of PC3), while absorbances at 1,060, 1,034, and 1,090 cm$^{-1}$ are enriched in the epidermal tissues (Fig. 2, F–H). The absorbance at 1,060 cm$^{-1}$ is dominated by, but not unique to, cellulose, whereas the latter two absorbances are selected as potentially diagnostic for the presence of glucomannans (Kacuráková et al., 2000).

### Immunogold Localization of β-Glucans

We confirmed the distribution of the β-glucan by immunogold labeling. Three-day-old maize coleoptiles were fixed for low-temperature embedding and immunogold labeling. A monoclonal antibody that recognizes β-glucan specifically and does not cross react with either cellulose or callose (Meikle et al.,

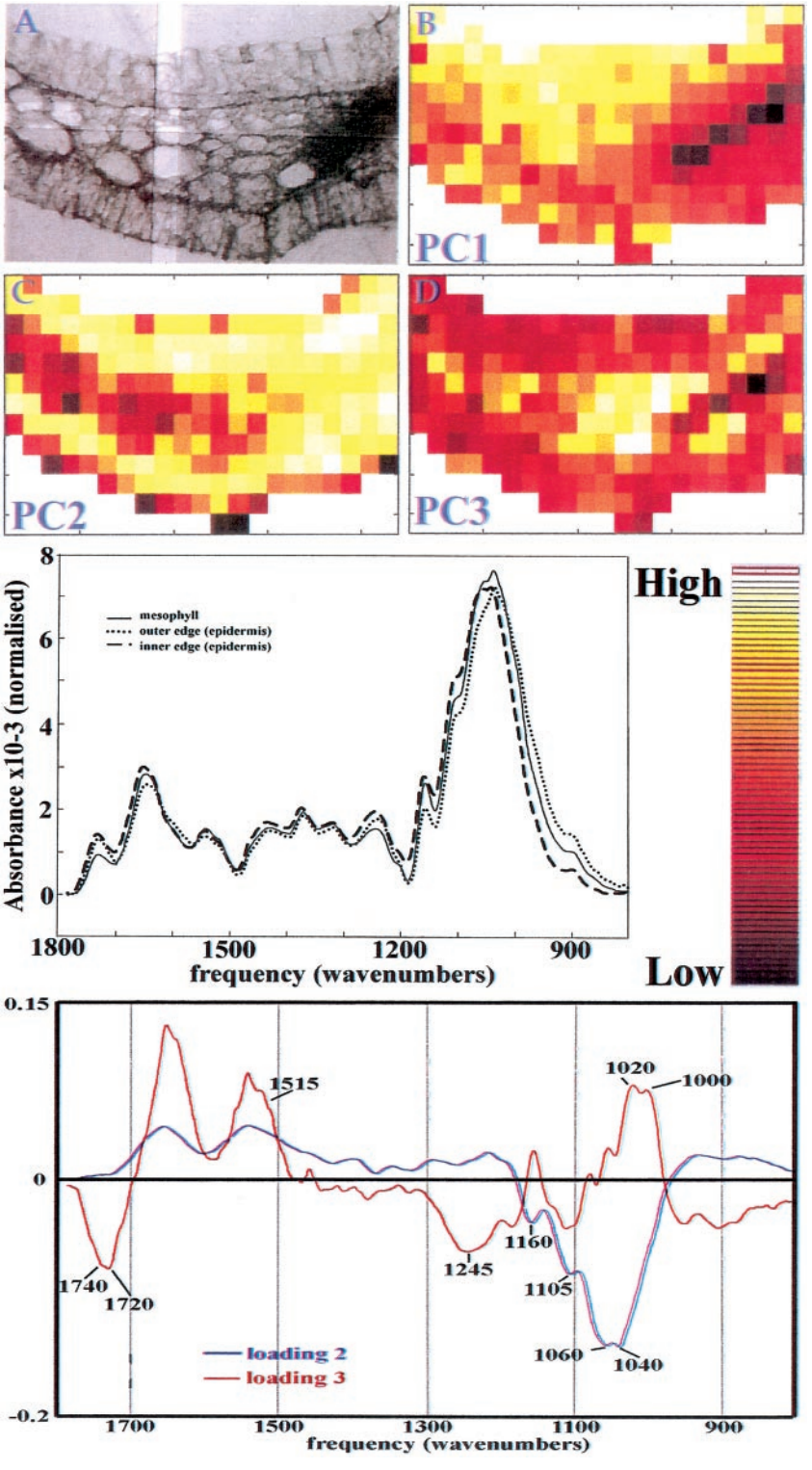


**Figure 1.** A, Brightfield micrograph of the coleoptile section using mirror optics in the IR microscope. An example of the area from which IR data is sampled is delimited by a pair of double-bladed apertures. B–D, Calculated scores of principal component (PC) 1, PC2, and PC3, respectively, displayed as chemical images. Middle, Average spectra of mesophyll cells, and the inner and outer edges of the outer epidermis are different from each other. The color gradient used in chemical images in Figures 1 and 2 corresponding to peak intensities is shown on the right. Bottom, Corresponding loadings for PC2 and PC3 with peaks of interest marked.

1994) densely labeled the mesophyll primary walls and inward-facing wall of the epidermis (Fig. 3, B, D, and E). Large regions of wall material between the cells were not labeled, comprising the middle lamellae and perhaps also the older, previously deposited primary wall (Fig. 3, B–D). The $\beta$-glucan was absent from the loose fibrillar matrix lining the cell corners (Fig. 3B). In the thick, outward-facing wall of the epidermis, the label was concentrated in the innermost strata of the wall nearest the plasma membrane, with decreasing amounts outward and little observed in the faintly stained region next to the cuticle

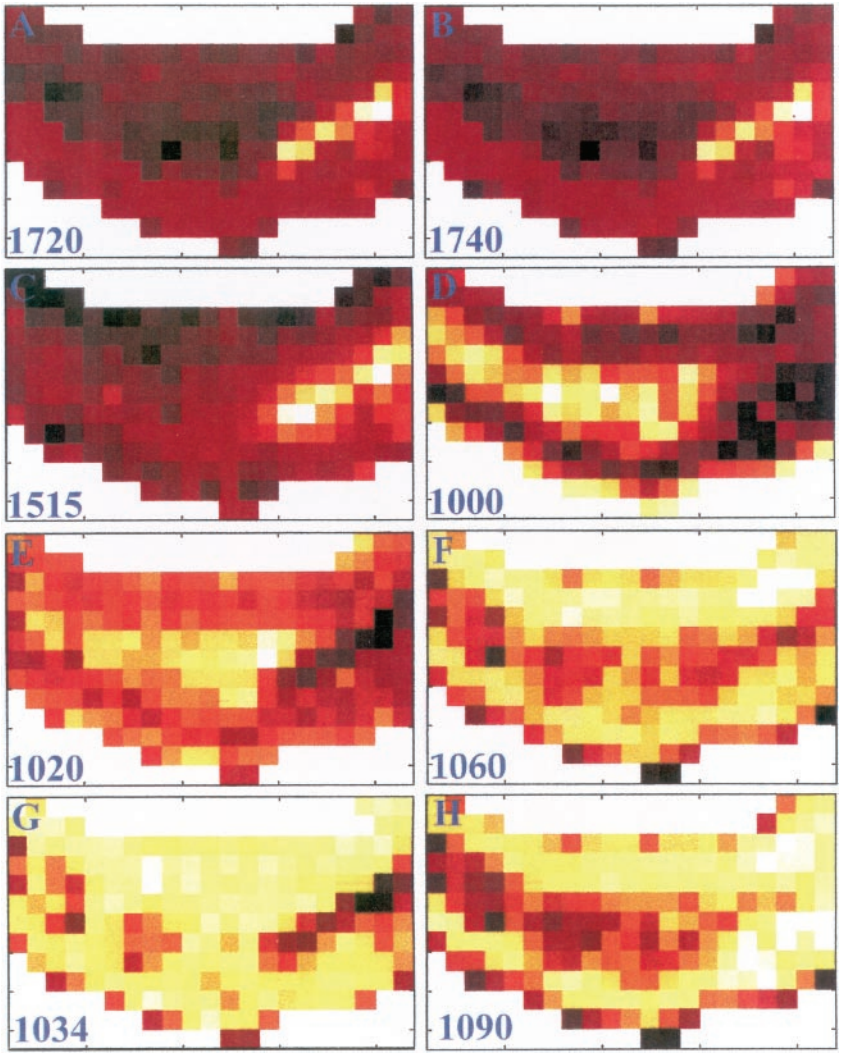


**Figure 2.** Chemical images of a transverse section of three-d-old coleoptile derived from FTIR spectra sampled with a 25- × 25-$\mu$m window. A, Phenolic esters sampled at 1,720 $cm^{-1}$. B, Carboxyl esters of uronic acids sampled at 1,740 $cm^{-1}$. C, Aromatic substances sampled at 1,515 $cm^{-1}$. D, Absorbance intensity at 1,000 $cm^{-1}$ sampled from PC3. E, Absorbance intensity at 1,020 $cm^{-1}$ sampled from PC3. F, Absorbance at 1,060 $cm^{-1}$ characteristic of cellulose. G and H, Absorbances at 1,034 and 1,090 $cm^{-1}$ respectively, characteristic of glucomannan.

(Fig. 3A). These labeling patterns were observed in tissues sampled both from the tip region and midsection of the coleoptile (data not shown). Quantitation of gold particles from a total area of 250 $\mu m^2$ in the electron micrographs reveals the highest labeling density in the outer epidermal wall (3,970 ± 450 particles per $\mu m^2$) to be only about two-thirds that of the mesophyll walls (6,460 ± 1,330 particles per $\mu m^2$). The density of particles fell markedly toward the outer lamellae of the epidermal wall, and very few were detected in the outermost 300 nm (Fig. 4).

### Sequential Extraction and Chemical Analyses of Wall Components from Epidermal Peels

Because epidermal peels could be isolated relatively easily, we further defined the architecture of this tissue. Extraction of epidermal peels floating on the surface of the reagents was carried out using 20 mM cyclohexane diamine tetraacetic acid (CDTA), a chelating agent, and 0.1 M NaOH to remove polymers possibly esterified to the wall matrix, acidified sodium chlorite, which oxidizes aromatic rings, and $\beta$-glucan endohydrolase, which hydrolyzes $\beta$-glucan specifically. The extractants and enzyme were used either singly or in combination to determine the relationship of the polymers dependent upon their specific chemical interactions. Treatment with 20 mM CDTA or sodium chlorite removed very little material from the epidermal walls. Sugar analyses (Table III), confirmed by methylation analyses (not shown), show that 0.1 M NaOH extracts only 67 $\mu$g per mg of total epidermal wall, primarily the highly substituted GAX and glucomannan. Chlorite treatment alone extracted insufficient material for methylation analysis, but was composed of Xyl, Glc, Ara, and a small amount of Man. However, extraction with 0.1 M NaOH after chlorite treatment yielded over one-half of the non-cellulosic material from the wall (Table III), and methylation analysis of this material shows it to be mostly GAX with a lower degree of branching, glucomannan, and a small amount of $\beta$-glucan (not shown). Treatment of the control cell walls with $\beta$-glucan endohydrolase released material comprising

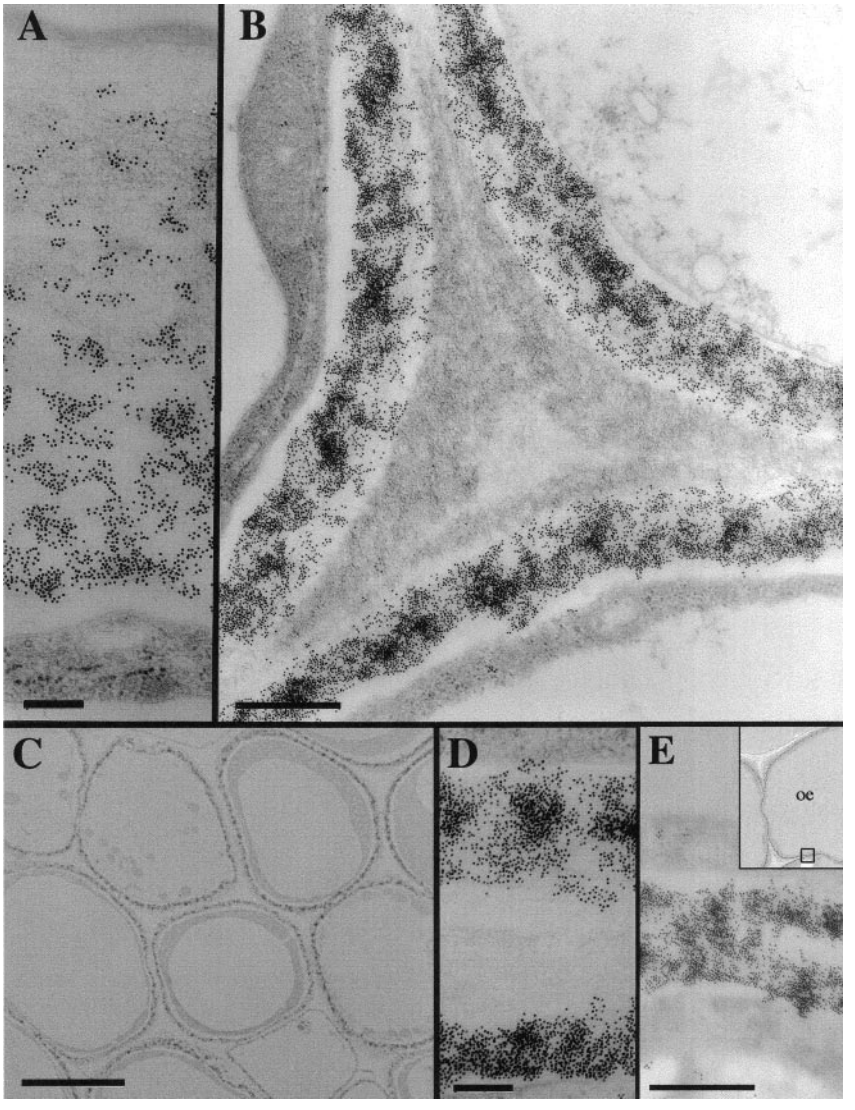


**Figure 3.** Immunolocalization of β-glucans in mesophyll cells and epidermis of developing maize coleoptiles using 10 nm colloidal gold-conjugated secondary antibody. A, The gradient of β-glucans immunolocalized in the outer wall of the epidermis. The cuticle is at the top of the figure, cytoplasm at the base. Scale bar represents 200 nm. B, β-Glucan epitopes are excluded from the cell corner formed by three mesophyll cells. Scale bar represents 500 nm. C, Low magnification image showing the immunostain in a sharply defined region of the wall closest to the plasma membrane of cells. Scale bar represents 5 μm. D, β-Glucans immunolocalized in two neighboring mesophyll cell walls but excluded from the middle lamella and older regions of wall. Scale bar represents 200 nm. E, β-Glucans immunolocalized uniformly across the inward-facing wall of the epidermis. Scale bar represents 200 nm.

90 mol % Glc (Table III), consistent with the subsequent detection by HPAEC-pulsed-amperometric detection of mostly the cellodextrin-(1→3)β-Glc oligomers diagnostic of β-glucan (Table II). Based on selective hydrolysis with the β-glucan endohydrolase, about 70% of the β-glucan still remained associated with the wall after extraction of over one-half of the non-cellulosic material by chlorite and NaOH (Table III).

### FTIR Spectroscopy of Epidermal Peels

FTIR spectra were obtained from three 150- × 150-$\mu m^2$ regions of the peels and triplicate averaged for each of a minimum of 20 coleoptiles per treatment. Extraction with acidic sodium chlorite makes little difference to the appearance of the spectrum of untreated material (Fig. 5, A and B), although the phenolic peak at 1,515 $cm^{-1}$ is absent in the chlorite-treated material. Extraction with 0.1 M NaOH lowers the ester absorbances at 1,734 and 1,250 $cm^{-1}$ substantially and affects the fingerprint region (1,200–900 $cm^{-1}$; Fig. 5C). Sequential extraction with acidic sodium chlorite followed by NaOH removed more esters (Fig. 5D). After further extraction of this material with the β-glucan endohydrolase, all of the remaining ester absorbance is removed and the carbohydrate region of the spectrum is dominated by absorbances that can be assigned to cellulose (1,160, 1,105, 1,056, and 1,039 $cm^{-1}$; Tsuboi, 1957; Liang and Marchessault 1959; Fig. 5E). Digital subtraction is necessary to reveal other features of the wall that have been modified by extraction with chlorite, NaOH, and β-glucan endohydrolase (Fig. 5, F–I). The digital subtraction spectrum shows that chlorite extraction removes very little material (Fig. 5F), whereas the NaOH treatment removes methyl ester (1,734 and 1,246 $cm^{-1}$), phenolic material (1,630 and 1,515 $cm^{-1}$), and some carbohydrate (positive and negative peaks between 1,200 and 900 $cm^{-1}$; Fig. 5G).

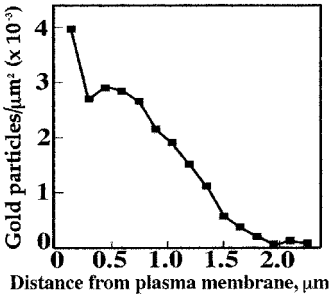


**Figure 4.** Quantitation of β-glucan density across the outer epidermal wall of developing maize coleoptile, using percentage area covered by gold particles conjugated to the secondary antibodies as a measure of relative epitope density. The graph shows number of gold particles per unit area as a function of perpendicular distance from the plasma membrane.

The sequential extraction using chlorite followed by hydroxide is very similar to hydroxide alone (Fig. 5, G and H). Further extraction with the β-glucan endohydrolase removes more esters and carbohydrates (Fig. 5I).

### Imaging of Epidermal Peels by FESEM

Incubation of floating epidermal peels on the surface of solutions containing chemical extractants selectively removed polymers and cross-linking compounds of known composition. The outer epidermis can be peeled without cell damage from the coleoptile and floated, cuticle side up, on any desired bathing solution. Hence, the cuticle side affixes to glass coverslips, which are then flipped over, air dried, and imaged by FESEM. After transfer to the surface of water, the peels were lifted onto specimen stubs such that the surface that had been in contact with the solution was uppermost for imaging in the FESEM. The FESEM technique allows extremely large areas of the sample to be observed, such as an entire epidermal peel (Fig. 6A). The orientation of cellulosic microfibrils in relation to the shape and position of the cell within a tissue, such as in an elongation zone, can be determined. Few surface features could be observed in unextracted peels, and a calcium chelating agent, either imidazole or CDTA, did not improve this (data not shown). Extraction with acidic sodium chlorite to oxidize phenolic substances within the wall or with 0.1 M NaOH to extract pectins and highly substituted arabinoxylans revealed long fibers embedded in a matrix material of uniform appearance (Fig. 6, B and C). By scanning from the tip to the base of the epidermal peel, no net orientation of these surface microfibrils was observed. However, these represent the outermost, and therefore oldest, microfibrils deposited within the wall, and changes may be occurring in regions closer to the plasma membrane. Sequential extraction by acidic sodium chlorite followed by 0.1 M NaOH reveals pores within the structure (Fig. 6D), and microfibril diameter is measured as between 13 and 20 nm, taking into account an estimated 2 to 4 nm of sputter coating with platinum. Removal of the matrix portion of the wall reveals up to six microfibrillar lamellae. It is not possible to determine the total number of lamellae in this en face view of the wall, given that

**Table III.** *Soluble and cell wall monosaccharide distributions after digestion or extraction of epidermal peels of the elongating maize coleoptile*

tr, Trace amounts below 0.2%; nd, not detected. Insoluble remainder represents the non-cellulosic cell wall monosaccharides remaining after enzymic digestion and/or chemical extraction. Soluble fractions from chemical extractions were neutralized and dialyzed extensively with water before freeze drying. Values in brackets are the yields of material in micrograms per milligram of epidermal wall (about 400 μg total non-cellulosic material per mg). Endoglucanase soluble represents monosaccharide released from enzymic digestion of the total wall, whereas [− $NaClO_2$ − NaOH]- endo soluble represents monosaccharide released from insoluble wall material remaining after chlorite and NaOH extraction.

| Sample | Monosaccharide | | | | | | |
|---|---|---|---|---|---|---|---|
| | Fuc | Rha | Ara | Xyl | Man | Gal | Glc |
| | | | | *mol %* | | | |
| Soluble fraction | | | | | | | |
| $NaClO_2$ soluble [23] | nd | tr | 24.1 | 28.5 | 15.1 | 3.8 | 28.7 |
| NaOH soluble [67] | tr | 1.1 | 29.4 | 36.4 | 10.6 | 4.0 | 18.3 |
| $NaClO_2$ + NaOH soluble [217] | 0.3 | 1.2 | 35.6 | 42.1 | 4.0 | 5.2 | 11.6 |
| Endoglucanase soluble [66] | nd | nd | 1.5 | 1.3 | 2.0 | 5.8 | 89.5 |
| [− $NaClO_2$ − NaOH]- endo soluble [54] | nd | 0.7 | 9.8 | 10.8 | 0.3 | 5.3 | 73.2 |
| Insoluble remainder | | | | | | | |
| Total wall | 0.5 | 2.7 | 29.0 | 37.5 | 3.0 | 6.9 | 20.4 |
| − 20 mM CDTA | 0.4 | 2.1 | 31.0 | 39.9 | 2.5 | 5.9 | 18.1 |
| − CDTA − endoglucanase | tr | 1.5 | 33.8 | 45.6 | 2.6 | 6.5 | 10.0 |
| − 0.34 M $NaClO_2$ | 0.3 | 3.2 | 30.2 | 39.2 | 2.7 | 5.4 | 18.8 |
| − 0.1 M NaOH | 0.3 | 1.6 | 27.7 | 37.7 | 2.8 | 6.5 | 23.3 |
| − $NaClO_2$ − NaOH | 0.2 | 1.9 | 23.8 | 35.0 | 3.0 | 7.0 | 29.1 |
| − $NaClO_2$ − NaOH − endoglucanase | 0.3 | 2.1 | 23.9 | 40.7 | 3.9 | 8.7 | 20.4 |

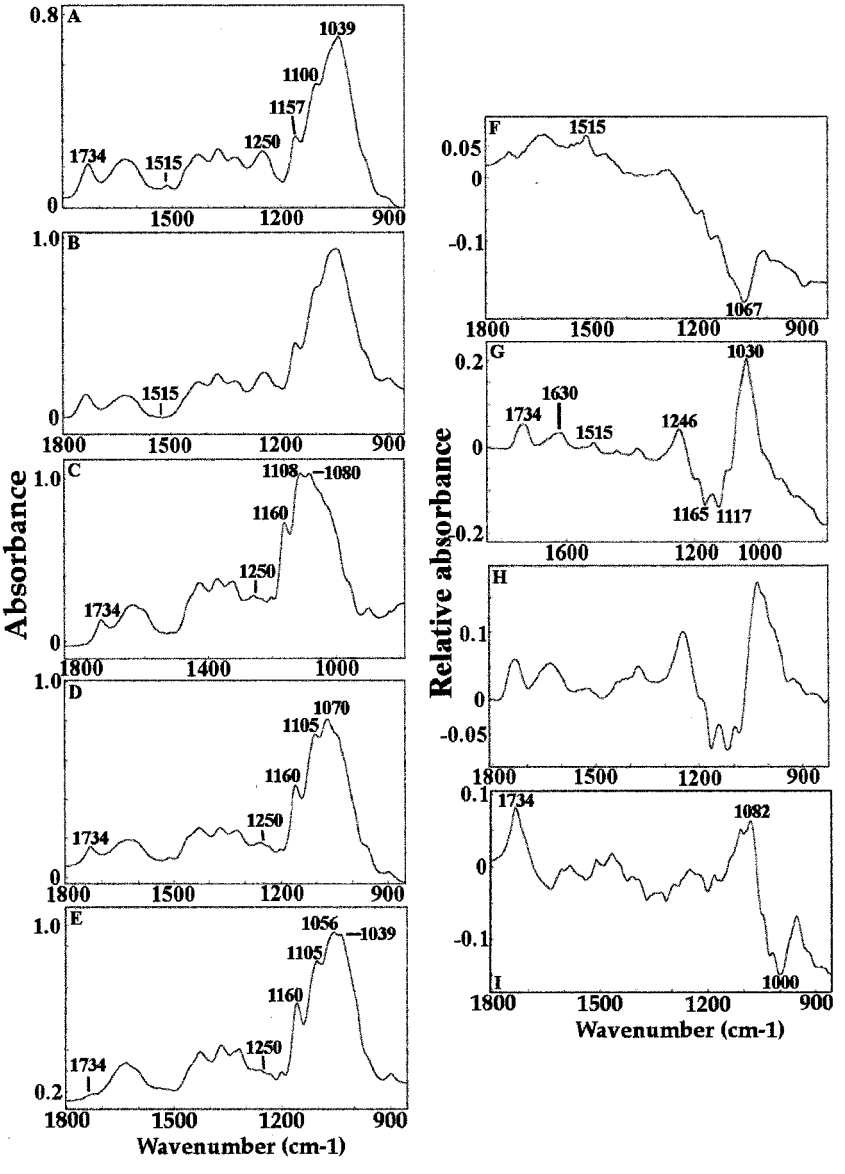


**Figure 5.** FTIR spectra of epidermal peels extracted with hot water (A), chlorite (B), NaOH (C), chlorite followed by NaOH (D), chlorite followed by NaOH followed by β-glucan endohydrolase digestion (E), and the results of digital subtractions between digital subtractions between control and chlorite (F), control and NaOH (G), control and chlorite + NaOH (H), and control and chlorite + NaOH + β-glucan endohydrolase (I). Peaks of interest are marked.

the wall thickness of these cells is about 250 nm in transmission electron micrographs of sections of coleoptiles. Treatment of this material with β-glucan endohydrolase does not further increase the porosity (Fig. 6E), even though β-glucan is distributed throughout the inward-facing epidermal wall (Fig. 3E).

Our observations from FESEM of epidermal peels after sequential extractions demonstrate that the polymeric material extracted by chlorite followed by NaOH constitutes the majority of the architectural material between the microfibrils. The material that has been extracted from between the microfibrils is largely GAX, glucomannan, and the small amount of pectin, whereas the material remaining bound to the microfibrils but not imaged as distinct polymers is β-glucan, glucomannan, and relatively less branched GAX (Table III).

## DISCUSSION

### Mesophyll Walls Have a Different Composition from Epidermal Walls

Although we have a good catalog of the kinds and distribution of cellulose and non-cellulosic polysaccharides, and phenolic substances that cross link them in the maize coleoptile (Carpita, 1996), our understanding of the polysaccharide composition is based solely on preparations containing mixtures of epidermis, mesophyll cells, and cells of the vasculature. We have investigated a novel microspectroscopic technique, called chemical imaging, to provide a closer correspondence between chemistry and tissue morphology (Figs. 1 and 2). We used exploratory PCA on the entire spectral data set to highlight contrast in the chemical image of a coleoptile tissue

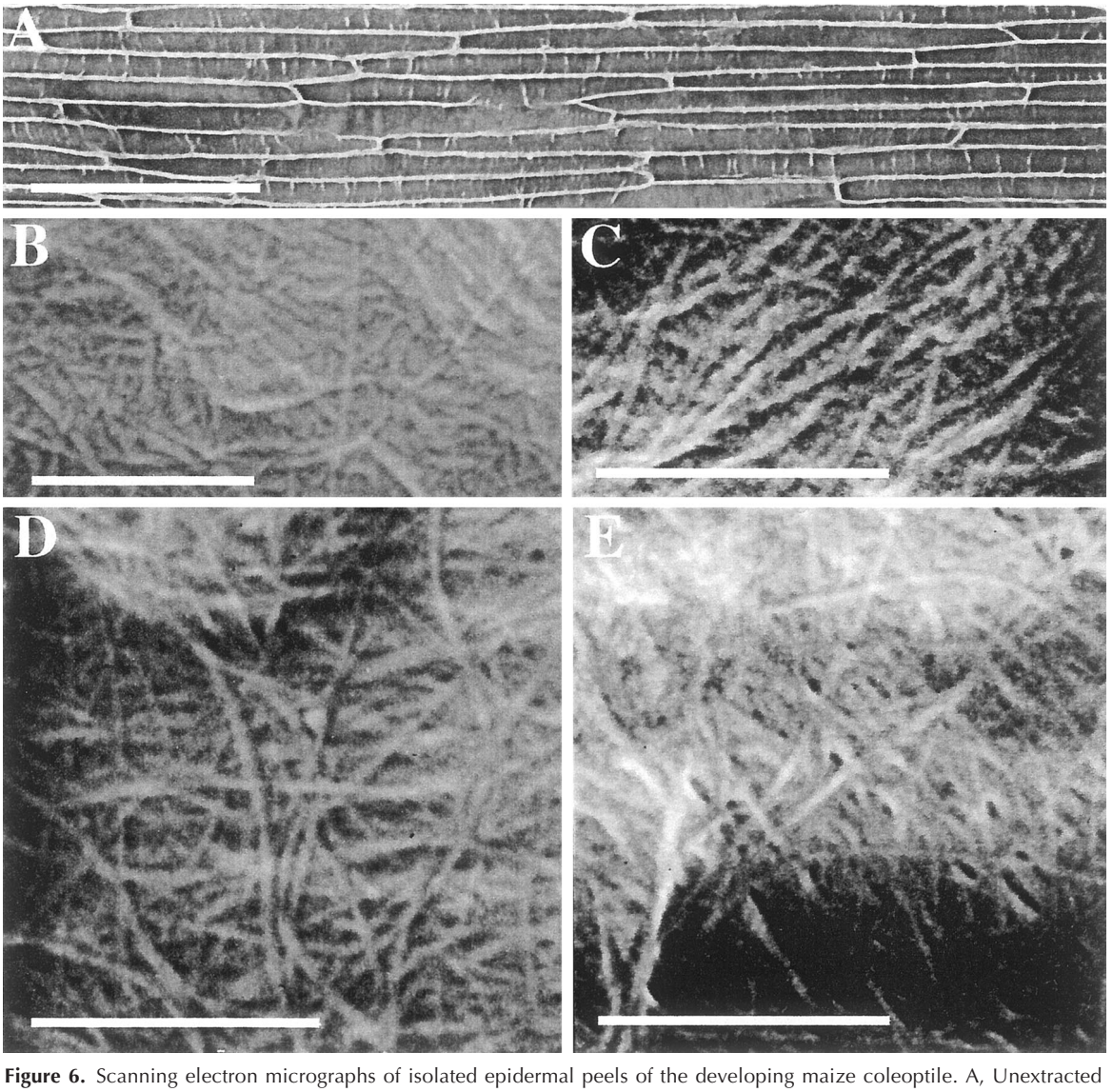


**Figure 6.** Scanning electron micrographs of isolated epidermal peels of the developing maize coleoptile. A, Unextracted epidermal peel at low magnification. B, Chlorite-extracted mesophyl walls, C, NaOH-extracted epidermal peel. D, Chlorite followed by NaOH extracted peel. E, Chlorite + NaOH-extracted peel digested with the $\beta$-glucan endohydrolase. Scale bar in A represents 200 $\mu$m, all other scale bars represent 500 nm.

section. The results from chemical imaging are consistent with chemical data in revealing the cellular distribution and relative abundance of ester groups, phenolics, and carbohydrates.

In this study, chemical imaging indicated that the mesophyll layer contained less methyl or phenolic ester, and less phenolic ring compounds, than the epidermis and vasculature, and contained different proportions of some carbohydrate components (absorbances at 1,000, 1,020, 1,034, 1,060, and 1,090 $cm^{-1}$). Methyl ester is slightly more abundant in the outer epidermis, and a colorimetric assay shows the polysaccharides in the outer epidermis to have an 82% degree of esterification compared with 75% in the mesophyll tissue. Phenolic compounds are expected in vascular tissue as a consequence of lignification. Distribution of absorbances at 1,034- and 1,090-$cm^{-1}$ peak were selected as characteristic for glucomannan (Kacuráková et al., 2000), and the chemical images both show enrichment in the epidermal tissue, consistent with sugar and linkage analyses. However, the chemical images are not identical, indicating that other absorbing species are present at these wavenumbers. The peaks at 1,000 and 1,020 $cm^{-1}$ were selected from the appropriate loadings and are not currently able to be assigned to specific polysaccharides.

There is more than twice as much cellulose in the epidermis than in the mesophyll (Table II) and the peak at 1,060 $cm^{-1}$, dominated by, but not unique to, cellulose, in chemical images is enriched in the epidermis. However, the PC loading 3, which contains spectral features of cellulose, is not similarly enriched in the epidermis. One explanation for this is that,

although cellulose content is considerably lower in the mesophyll, the β-glucan concentration is nearly 4-fold greater. The similarity of the spectra of cellulose and β-glucan (data not shown) means that the reduction of one component is spectrally compensated for by the increase of the other. Thus, the chemical image of PC3 is the result of other compositional changes and the subtle spectral differences between cellulose and the mixed-linkage β-glucan. We have not constructed chemical images of the distributions of β-glucan and GAX because overlapping absorbances with other polymers, particularly cellulose, make unambiguous assignment of single peaks problematic. The application of chemical imaging to biological specimens is in its infancy, but as better peak assignments are found by the methods and examples we describe here, it may become possible to map the distribution of specific molecules in tissue sections.

We examined the physical and biochemical distinctions between mesophyll and epidermal walls. The outer-facing epidermal wall is over 2 μm thick compared with the 250-nm-thick walls of the mesophyll cells and inner-facing wall of the epidermis (Fig. 3, A, D, and E). In epidermal walls, cellulose comprises about 60% of wall mass, compared with about 30% in the mesophyll walls (Table II). The non-cellulosic polysaccharides of epidermal walls are similar to those of mesophyll walls (Table I) with large amounts of GAX, and smaller amounts of other matrix glycans and pectic substances (Tables I and II). The principal differences were the enhanced amounts of glucomannans in epidermal cell walls, and an enhancement of the β-glucan in the mesophyll cell walls, about 4-fold higher than in epidermal walls (Table II). Meikle et al. (1994) demonstrated the specificity of the monoclonal antibody BG1 against cereal mixed-linkage β-glucans, and found this epitope to be distributed uniformly across the aleurone walls of wheat (*Triticum aestivum*) endosperm cells but excluded from the middle lamella. The β-glucan is distributed uniformly across the thin walls of the mesophyll cells, whereas it is concentrated primarily on the innermost portion of the outer facing wall of the epidermis (Fig. 3, A and D). Similar to the distribution in wheat aleurone, the β-glucan is present only in the primary wall and absent from middle lamellae and cell corners (Fig. 3, B–D). The density of the gold particles in the mesophyll wall is about twice that of highest concentration of the epidermis. β-Glucan is increasingly abundant closer to the plasma membrane and absent from an outer domain just underlying the cuticle that contains lightly stained fibrillar material (Figs. 3A and 4). In contrast, β-glucan is distributed across the entire wall of the inner-facing wall of the epidermal cells (Fig. 3E).

### Architecture of the Epidermal Walls of Maize Coleoptiles

The fast-freeze rotary shadow replica technique has previously been used to directly visualize cell wall architecture of dicotyledonous species (McCann et al., 1990; Fujino et al., 2000). The images obtained are thought to preserve the native architecture of cell walls, and many thin cross-linking fibers are visible as well as cellulosic microfibrils. However, the sample preparation required for this technique is extensive and the area of replica from which useful images can be obtained is small. The development of the field emission gun makes it possible to visualize native cell walls at resolutions adequate for measuring microfibril diameter, orientation, and spacing in the SEM with little or no sample preparation (Sugimoto et al., 2000). A further advantage of this technique is that large areas of the sample can be imaged at high resolution. In this study, we have been able to image walls from a substantial portion of the length of an epidermal peel, about 2 cm (Fig. 6A). We applied FESEM to observe the architecture of the outermost strata of the epidermal wall facing the mesophyll cells of the coleoptile.

We established previously that dilute NaOH extracts primarily a highly substituted GAX from the walls of the maize coleoptile (Carpita, 1983a; Carpita and Whittern, 1986) and treatment of walls with acidic sodium chlorite eliminates the cross linking of arabinoxylans by the aromatic substances but extracts little polysaccharide (Carpita, 1983b). However, when the polyphenolic network is broken by oxidation in acidic chlorite, the dilute NaOH extracts a majority of the GAX, indicating that a significant amount of the wall matrix polymers are held in a matrix by the aromatic substances (Carpita, 1983b, 1986). Despite the marked differences in wall thickness, and the proportions of cellulose, β-glucan and glucomannan, this extraction behavior was observed for both mesophyll and epidermal cells. Also, β-glucan endohydrolase treatment to specifically digest β-glucans released primarily Glc from both epidermal and mesophyll cells. About 70% of the enzyme-digestible β-glucan in both epidermal and mesophyll walls was retained in the wall matrix after chlorite + NaOH extraction (Table III), indicating that these molecules are not held solely by aromatic cross linkages and constitute little of the matrix material between the microfibrils (Fig. 6E). The observation of a selective release of glucomannan under gentle extraction is consistent with the extraction of this polymer from isolated coleoptile walls with urea (Carpita, 1983b).

The FESEM images of the epidermal walls after chemical extraction or enzyme digestion permit an insight into the architectural roles of different matrix polymers. In control epidermal peels, the microfibril impressions could be seen through a dense blanket of intervening matrix material (Fig. 6B). The chelator CDTA removed a small amount of pectic substances and highly substituted GAX (not shown), and chlorite treatment released a small amount of highly substituted GAX and glucomannan (Table III), but nei-

ther CDTA nor chlorite treatment alone substantially altered the appearance of the wall (Fig. 6B). This finding contrasts with observations of onion (*Allium cepa*) parenchyma walls, where imaging of the microfibrillar matrix is enhanced markedly by removal of chelator-soluble pectins (McCann et al., 1990). These differences in wall appearance after chelator extraction are consistent with the findings that the pore size of pectin-rich type I walls are controlled largely by the pectin matrix (Baron-Epel et al., 1988), whereas that of the pectin-poor, GAX-rich type II walls is not (Titel and Ehwald, 1999).

Dilute NaOH removed some of the material between microfibrils, improving their visualization (Fig. 6C). From our chemical analyses, which are fully consistent with previous work, the major polysaccharides released are the highly substituted GAX and a small amount of glucomannan (Table III; Carpita, 1983a, 1983b). Oxidation of the aromatic cross-linking framework of the wall with chlorite released very little water-soluble polysaccharide. FTIR spectroscopy confirmed that phenolic absorbances were removed by chlorite treatment, whereas dilute NaOH removed methyl esters. However, extraction with chlorite followed by dilute NaOH permitted several lamellae of microfibrils in the wall to be imaged (Fig. 6D). Although loss of arabinosyl units ostensibly yields runs of unbranched xylan that can hydrogen bond to each other, treatment of the wall with NaOH subsequent to chlorite treatment removed large amounts of the GAX of various degrees of substitution (Table I; Carpita, 1983b). From these data, we deduce that GAXs are largely interconnected by aromatic residues and comprise the majority of the interstitial material between the microfibrils (Fig. 6, D and E).

The aromatic residues are largely ferulate and diferulate esterified to GAX, which are extracted completely by less than 0.5 M NaOH (Carpita 1986). Additional aromatic substances remain tightly bound and require much more concentrated NaOH to remove them. Scalbert et al. (1985) used NMR spectroscopy to show that a wheat straw aromatic fraction contains both ester- and ether-linked residues, with the ether-linked residues more strongly bound to the wall matrix. In maize coleoptiles, the content of aromatic substances is lowest during the highest rates of growth, and the content increases markedly, as much as 10-fold in some fractions, as growth wanes. Coincident with this, Pro and Hyp, present in vanishingly small amounts during growth, also increase as growth stops (Carpita, 1986). Müsel et al. (1997) confirmed these findings in a study of 5-d-old coleoptiles, and showed further that, in addition to the hydroxycinnamic acids, lignin-like substances (thioacidolysis positive) also constitute part of the aromatic composition. These data indicate that the aromatic residues and polysaccharides (GAX) form coextensive matrices with the highly substituted, GAX-rich interstitial matrix and the relatively unsubstituted GAX of the β-glucan and glucomannan-enriched microfibril coatings. Based on observations of a marked inverse relationship between either growth rate or auxin responsiveness and the accumulation of these substances in the maize coleoptile (Carpita, 1986), it is doubtful that polysaccharide-polyphenol dynamics play a major role in cell growth.

β-Glucan remains attached to the microfibrils even after extensive removal of the matrix material by chlorite/NaOH treatment (Table III). The residual wall material has a cellulose-like IR spectrum with characteristic features at 1,200, 1,160, 1,105, 1,056, and 1,039 $cm^{-1}$ (Tsuboi, 1957; Liang and Marchessault, 1959; Fig. 5E). Digestion of the β-glucan remaining after chlorite + NaOH extraction does not increase the wall porosity further (Fig. 6E). Hence, we deduce that about two-thirds of the β-glucans are tightly packed around the microfibrils. Thus, the model of the type II wall (Carpita and Gibeaut, 1993), in which both GAX and β-glucans are depicted as cross-linking glycans binding to and bridging between microfibrils, requires some revision. For this growth-specific stage of coleoptile development, our data support a model in which β-glucan, interlaced by GAX of low degree of substitution and glucomannans, is tightly associated with the microfibrils. GAX of higher degree of arabinosyl substitution and some glucomannan constitutes the major, pore-determining interstitial material between the microfibrils.

### Differential Architectural Roles for β-Glucan, Glucomannan, and GAX in Growth of the Coleoptile

The β-glucans of graminaceous species are one of the few developmental stage-specific polysaccharides known (Carpita, 1996). Virtually absent from meristematic cells, β-glucans begin to be synthesized at the onset of cell elongation, reach a maximum abundance during the most rapid phase of elongation, and are then largely degraded once elongation begins to wane (Kim et al., 2000). Because of this correlation, research for several decades has focused on these polymers and their direct involvement in wall extension (for review, see Carpita, 1996). A long-held idea is that the β-glucans, thought to have a role in cross-linking the cellulose microfibrils, are cleaved by an endo-β-D-glucanase, loosening the wall and allowing turgor-driven cell expansion (Huber and Nevins, 1981). Two observations support this hypothesis: exo- and endo-β-D-glucanase polypeptides and activities appear in cell walls during growth (Inouhe and Nevins, 1998), and polyclonal antisera that bind to these enzymes inhibit growth (Hoson et al., 1992). However, the mechanism by which the antisera inhibit growth has never been established satisfactorily, and the discoveries in growing grass tissues of xyloglucan endo-transglycosylase (Pritchard et al., 1993) and β-expansins (Cosgrove et al., 1997) have reopened the question of the necessity of β-glucan hydrolysis for

wall loosening during growth. The appearance of the exoglucanase in the wall is not correlated strictly with growth but rather the turnover of the β-glucan that occurs after growth has ceased (Kim et al., 2000). The endo- and exo-glucanase-catalyzed turnover of β-glucan may occur after the physical mechanism of wall loosening required for expansion and may be part of a sugar-recycling mechanism.

The ability to place β-glucans not only in a cell-specific manner but also in an architectural framework provides new information necessary to evaluate the direct role of the polymer in cell growth. Kutschera (1989) reviewed evidence that the epidermis controls the rate of elongation, whereas the underlying mesophyll cells expand coordinately in a passive manner. Hoson et al. (1992) demonstrate a slight lowering of elongation rate in the presence of polyclonal antibodies against β-glucan but only if they are permitted to infiltrate the outer epidermis. Our immunocytochemical detection of β-glucan shows that the polymer is largely confined to the inner portions of the outward facing epidermal wall (Fig. 3A), where wall tension is calculated to be at a maximum (Richmond, 1983). The gradient of β-glucan content across the epidermal wall could arise either because the glucan is synthesized and deposited to a greater extent at the inner wall at this stage of development or because a gradual hydrolysis occurs from the outer wall inward. The β-glucan content of the mesophyll cells is at least twice that of the highest enrichment in the epidermis, and there is no evidence of a gradient across the wall, although the epitope is clearly absent from the middle lamellae and cell corners. Regardless of relative abundance between mesophyll cells and epidermal cells, the β-glucans of the outer epidermal wall are localized where load-bearing stresses are predicted to occur.

Our previous model of the type II walls of grasses proposed a framework of cellulose microfibrils interlaced with GAX and β-glucan, which is then embedded in a matrix of highly substituted GAX and some pectins (Carpita and Gibeaut, 1993; Carpita, 1996). To develop models to predict how and where expansins and xyloglucan endo-transglycosylases might function in the wall, Cosgrove (1999), in his adaptation of an earlier model proposed by Talbott and Ray (1992), proposed a new model of wall architecture for the type I wall. In this model, the cellulose microfibrils are coated with a tightly associated matrix of glycans, mainly xyloglucans, with which is associated a looser matrix of xyloglucans and other matrix glycans that interlaces adjacent xyloglucan-coated microfibrils and a pectin "filler." Our FESEM investigations lend support for a similar model for the type II wall of grasses but with different components. A combination of chlorite + NaOH removes most of the matrix material between microfibrils (Fig. 6D), but no more than 30% of the β-glucan (Table III). Digestion of β-glucan by the specific endohydrolase alone does not alter the matrix structure, and digestion subsequent to chlorite + NaOH extraction does not alter the microfibril appearance or spacing (Fig. 6E). Although relatively low in abundance compared to other non-cellulosic polysaccharides, glucomannans, and homogalacturonans are the only polymers in greater abundance in the epidermal cells compared to the mesophyll-enriched cell walls (Table II), and glucomannan appears in fractions tightly associated with cellulose as well as those loosely associated with the matrix (Table III). Hence, we deduce the structure of the grass type II wall to consist of cellulose microfibrils with tightly adherent β-glucans, low-substituted GAX and glucomannans, and the microfibrils densely coated in these polysaccharides are embedded in a matrix of mostly highly substituted GAX and additional glucomannan and pectic substances. The molecular interactions relevant to growth kinetics may be those between the β-glucans and glucomannans coating the microfibrils and the GAX-rich material in the intervening spaces. Thus, it is the presence of β-glucans coating the microfibrils that function in wall dynamics during growth, not its hydrolysis. Wall reconstitution experiments with defined composites of cellulose and specific cross-linking matrix polymers showed that expansin increased the rate of strain of cellulose-xyloglucan composites, whereas cellulose-glucomannan composites were unaffected by such treatment (Whitney et al., 2000). Nevertheless, how several growth-relevant polysaccharides interact to make an extensible matrix needs further evaluation. Control of extension growth may require two coordinated mechanisms of displacement to allow wall slippage—one to dissociate the surface-associated polymers and one to affect rearrangement of the matrix material as a whole.

## MATERIALS AND METHODS

### Plant Material

Maize (*Zea mays*) hybrid seeds obtained from Asgrow Seeds (Kentland, IN), were soaked overnight in water bubbled with air at ambient temperature, sown in moist vermiculite, and incubated in darkness at 30°C for an additional 60 to 64 h. The coleoptiles are about 3.5 cm long at this stage, having just transited the midpoint of elongation. The epidermal layers were peeled with watchmaker's forceps and floated cuticle side up on deionized water. Any adhering mesophyll tissue was excised with a pair of microscissors. In some instances, the epidermal peels, and mesophyll cells devoid of their outer epidermis, were also collected in absolute ethanol for preparation of cell wall material by extractions described below. The tips and central portions of some coleoptiles were fixed for low-temperature embedding.

### Extraction Methods

For sequential extractions, the epidermal peels were floated on the extraction media. Control peels were heated to 65°C in deionized water for 1 h. Some of the epidermal

peels and isolated mesophyll walls were processed immediately for FESEM or FTIR, whereas pectic substances were extracted from the remainder by transfer to either 2 M imidazole[HCl], pH 7 (for FESEM only), or 100 mM CDTA in 20 mM potassium phosphate, pH 7, for 1 h each at ambient temperature. Depectinated peels and mesophyll walls were washed with water, and some of the samples were transferred to either 0.34 M $NaClO_2$ in 65 mM acetic acid for 1 h at 65°C or directly to 0.1 M NaOH (containing 3 mg $mL^{-1}$ $NaBH_4$) for 1 h at ambient temperature. Some of the chlorite-treated peels and mesophyll walls were washed briefly with water and transferred to 0.1 M NaOH + borohydride for 1 h. Following sequential extractions by chlorite and NaOH, peels and mesophyll walls were washed with water and 1 mL of 50 mM Na acetate, pH 5.5, added to slightly acidify the suspension or floating solution, and then with additional water to neutrality. Samples of control and chlorite and NaOH-treated peels were incubated with a *Bacillus subtilis* (1→3),(1→4)-β-D-glucan endo-4-glucohydroase (EC 3.2.1.73), which specifically digests the mixed-linkage β-glucans (Anderson and Stone, 1975), for 3 h at 37°C. The enzyme was purified from a commercial preparation from Novo *Ban*I20 (Novo Laboratories, Wilton, CT) by batch elution from DEAE-cellulose and gel permeation chromatography on Bio-Gel P-60 essentially as described by Kato and Nevins (1984) and stored frozen at −20°C. The enzyme is now commercially available from Biosupplies Australia Ltd. (Parkville 3052, Australia). The peels were then washed with several changes of deionized water. At least 30 peels representing each treatment were obtained for FTIR and biochemical studies. For the biochemical studies, the soluble fractions from the NaOH and chlorite + NaOH were collected, acidified with glacial acetic acid, dialyzed extensively against deionized water, and freeze dried.

The additional epidermal peels and isolated mesophyll cells collected in absolute ethanol were heated to 65°C for 1 h, rinsed with water, and homogenized in a glass-glass grinder (Kontes-Duall, Thomas Scientific, Swedesboro, NJ) in 1% (w/v) SDS in 50 mM Tris[HCl], pH 7.2. The cell walls from the homogenate were collected on a nylon mesh filter to remove all cytosolic debris and starch grains (47-μm pore size, Nitex, Briarcliff Manor, NY), and washed sequentially with water, methanol, and water. The walls were suspended in deionized water and allowed to settle. Aliquots of these wall preparations were then subjected to the extractions and the β-glucan endohydrolase-digestion scheme, as described for the floated peels. Cellulose was determined independently as acetic-nitric acid-resistant material (Updegraff, 1969), with micrograms of Glc equivalent determined by a phenol-sulfuric assay (Dubois et al., 1956).

### Quantitation of Cell Wall Neutral Sugars, Pectic Substances and Their Esters, and Specific Polysaccharides

The esterified and unesterified uronic acid constituents were reduced in paired reactions with $NaBD_4$ and $NaBH_4$ to reveal the proportion of total esterified and unesterified uronic acid (Kim and Carpita, 1992, as modified by Carpita and McCann, 1998). Uronic acids were assayed by a carbazole-sulfamate assay (Filisetti-Cozzi and Carpita, 1991).

Portions of the walls and epidermal peels, and isolated polymers derived from them, were hydrolyzed with 2 M trifluoroacetic acid containing 1 μmol of *myo*-inositol for 90 min at 120°C. The trifluoroacetic acid was evaporated under a stream of nitrogen, and the sugars were converted to alditol acetates (Gibeaut and Carpita, 1991). The alditol acetates were separated by gas-liquid chromatography on an SP-2330 vitreous silica capillary column (0.25 mm × 30 m; Supelco, Bellefonte, PA). The oven temperature was programmed from 170°C to 240°C at 5°C $min^{-1}$ with a 6-min hold at the upper temperature. The neutral sugar composition was verified by electron-impact mass spectrometry (Carpita and Shea, 1989).

GAX, β-glucans, glucomannans, and pectic substances were quantified by linkage analysis deduced from separation of partly methylated alditol acetates (Gibeaut and Carpita, 1991) and determination of structure by electron-impact mass spectrometry (Carpita and Shea, 1989). Estimations of the amounts of each polymer per milligram of cell wall were made from a combination of non-cellulosic sugar analyses and quantitative linkage analyses based on known linkages of grass polysaccharides (as described in Carpita, 1984).

### High-Performance Anion Exchange High-Performance Liquid Chromatography

The mixed-linkage β-glucan content was quantified after hydrolysis with the β-glucan endohydrolase into diagnostic oligosaccharides, separation on a CarboPac-1 (Dionex, Sunnyvale, CA) HPAEC, and detection by pulsed amperometry (Buckeridge et al., 1999). Samples of 100 μL were injected onto the column equilibrated in 200 mM NaOH with a flow rate of 1.0 mL $min^{-1}$. The oligomers were eluted in a 20-min linear gradient of sodium acetate from 0 to 80 mM followed by a 10-min linear gradient to 200 mM. The signal was calibrated using cellobiosyl- and cellotriosyl-(1→3) β-D-Glc oligomers hydrolyzed from known amounts of authentic barley β-glucan.

### FESEM

The epidermal peels were either air dried on a coverslip or picked up with a piece of cellulose acetate paper, inverted onto the SEM stub, and frozen by plunging into liquid nitrogen slush at −210°C. The SEM micrographs were taken at 5 kV or below, using an XL30 FESEM (FEI UK Ltd., Cambridge, UK) fitted with a CT1500HF cryosystem (Gatan UK, Oxford), and recorded on FP4 120 roll film (Ilford, Mobberley, UK). Samples were routinely sputter-coated with 2 to 4 nm of platinum before imaging.

### Transmission Electron Microscopy and Immunocytochemistry

Tissue blocks of about 2 $mm^3$ were taken from the tip region and midsection of the 3.5-cm-long maize coleoptiles

and fixed overnight in 2% (w/v) glutaraldehyde in 0.1 M sodium cacodylate, pH 7.2, then low-temperature embedded as described previously (Wells, 1985; Hills et al., 1987). Thin sections (100 nm) were cut on an ultramicrotome (Leica, Milton Keyes, UK) and picked up on carbon-coated and plastic-filmed gold grids. Mixed-linkage β-glucans were detected with a monoclonal antibody that recognizes an authentic barley β-glucan (Meikle et al., 1994; available from Biosupplies Australia, Melbourne, Australia), visualized by a 10-nm colloidal gold-conjugated rabbit anti-mouse secondary antibody (Sigma, Poole, UK). The blocking solution was 1% (w/v) acetylated bovine serum albumen (Aurion, Wageningen, The Netherlands) in phosphate-buffered saline plus 0.1% (w/v) Tween 20, and incubation solution for washes was 0.1% acetylated bovine serum albumen in phosphate-buffered saline plus 0.01% (w/v) Tween 20. The number of gold particles per 250-$\mu m^2$ area of wall was estimated by digital imaging after scanning with an Epson QuickScan at 300 dpi, and the band intensities were quantified with an IP Gel image analysis program (Scanalytics, Vienna, VA) after contrast adjustments to specifically select only the gold particles.

### FTIR Microspectroscopy and Chemical Imaging

The epidermal peels were placed on 2-mm-thick × 13-mm-diameter barium fluoride windows, and the materials were air dried at 37°C for about 1 h. The windows were supported on the stage of a UMA500 microscope accessory of a FTS175c FTIR spectrometer (Bio-Rad, Hemel Hempstead, UK) equipped with a liquid nitrogen-cooled mercury cadmium telluride detector. An area of wall (150 × 150 μm) was selected for spectral collection in transmission mode. One hundred twenty-eight interferograms were collected with 8 $cm^{-1}$ resolution and co-added to improve the signal-to-noise ratio for each sample. Three spectra were collected from different areas of each epidermal peel and then averaged and baseline corrected. The triplicate-averaged spectra from a minimum of 20 to 60 epidermal peels per treatment were then averaged and used for digital subtraction.

For chemical imaging, transverse sections were hand cut from 3-d-old maize coleoptiles that were frozen in a cryosectioning medium (Tissue-Tek, Agar, Stansted, UK). Sections about 50 μm thick were picked up onto barium fluoride windows. The sections adhering to the surface were then washed extensively with water to remove all traces of the sectioning medium. A small amount of the sectioning medium was also streaked across a barium fluoride window as a control. An array of FTIR spectra was acquired with an aperture size of 25 × 25 μm with 8-$cm^{-1}$ resolution and with 128 co-added scans.

## ACKNOWLEDGMENTS

We thank Debbie Sherman (Purdue University Electron Microscopy Center, West Lafayette, IN) for digital quantitation of the immunolocalized polysaccharide epitopes, Breeanna Urbanowicz and Bethany Elkington (Purdue University) for alditol acetate analyses, and Sue Bunnewell (John Innes Centre, Norwich, UK) for photography. We are grateful to Marta Kacuráková (Institute of Food Research, Norwich, UK) for helpful discussions.

Received February 14, 2001; returned for revision April 12, 2001; accepted June 15, 2001.

## LITERATURE CITED

**Anderson MA, Stone BA** (1975) A new substrate for investigating the specificity of β-glucan hydrolases. FEBS Lett **52:** 202–207

**Baron-Epel O, Gharyal PK, Schindler M** (1988) Pectins as mediators of wall porosity in soybean cells. Planta **175:** 389–395

**Buckeridge MS, Vergara CE, Carpita NC** (1999) Mechanism of synthesis of a cereal mixed-linkage (1→3),(1→4) β-D-glucan: evidence for multiple sites of glucosyl transfer in the synthase complex. Plant Physiol **120:** 1105–1116

**Carpita NC** (1983a) Hemicelluloses of the cell walls of *Zea* coleoptiles. Plant Physiol **72:** 515–521

**Carpita NC** (1983b) Fractionation of hemicelluloses from maize cell walls with increasing concentrations of alkali. Phytochemistry **23:** 1089–1093

**Carpita NC** (1984) Cell wall development in maize coleoptiles. Plant Physiol **76:** 205–212

**Carpita NC** (1986) Incorporation of proline and aromatic amino acids into cell walls of maize coleoptiles. Plant Physiol **80:** 660–666

**Carpita NC** (1996) Structure and biogenesis of the cell walls of grasses. Annu Rev Plant Physiol Plant Mol Biol **47:** 445–476

**Carpita NC, Gibeaut DM** (1993) Structural models of primary cell walls in flowering plants: consistency of molecular structure with the physical properties of the walls during growth. Plant J **3:** 1–30

**Carpita NC, McCann MC** (1998) Some new methods to study plant polyuronic acids and their esters. *In* R Townsend, A Hotchkiss, eds, Progress in Glycobiology. Marcell Dekker, New York, pp 595–611

**Carpita NC, Shea EM** (1989) Linkage structure of carbohydrates by gas chromatography-mass spectrometry (GC-MS) of partially methylated alditol acetates. *In* CJ Biermann, GS McGinnis, eds, Analysis of Carbohydrates by GLC and MS. CRC Press, Boca Raton, FL, pp 157–216

**Carpita NC, Whittern D** (1986) A highly-substituted glucuronoarabinoxylan from developing maize coleoptiles. Carbohydr Res **146:** 129–140

**Chen L-M, Carpita NC, Reiter W-D, Wilson RW, Jeffries C, McCann MC** (1998) A rapid method to screen for cell wall mutants using discriminant analysis of Fourier transform infrared spectra. Plant J **8:** 375–382

**Cosgrove DJ** (1999) Enzymes and other agents that enhance cell wall extensibility. Annu Rev Plant Physiol Plant Mol Biol **50:** 391–417

**Cosgrove DJ, Bedinger PA, Durachko DM** (1997) Group I allergens of grass pollen as cell wall loosening agents. Proc Natl Acad Sci USA **94:** 6559–6564

**Dubois M, Gilles KA, Hamilton JK, Rebers PA, Smith F** (1956) Colorimetric method for the determination of sugars and related substances. Anal Chem **28:** 350–356

**Filisetti-Cozzi TMCC, Carpita NC** (1991) Measurement of uronic acids without interference from neutral sugars. Anal Biochem **197:** 157–162

**Fujino T, Sone Y, Mitsubishi Y, Itoh T** (2000) Characterization of cross-links between cellulose microfibrils, and their occurrence during elongation growth in pea epicotyl. Plant Cell Physiol **41:** 486–494

**Gibeaut DM, Carpita NC** (1991) Tracing the biosynthesis of the cell wall in intact cells and plants. Selective turnover and alteration of cytoplasmic and cell wall polysaccharides of proso millet cells in liquid culture and *Zea mays* seedlings. Plant Physiol **97:** 551–561

**Hills GJH, Plaskitt KA, Young ND, Dunigan DD, Watts JW, Wilson TMA, Zaitlin M** (1987) Immunogold localization of the intracellular sites of structural and nonstructural tobacco mosaic virus proteins. Virology **61:** 488–496

**Himmelsbach DS, Khahili S, Akin DE** (1999) Near-infrared-Fourier-transform-Raman microspectroscopic imaging of flax stems. Vib Spectrosc **19:** 361–367

**Hoson T, Masuda Y, Nevins DJ** (1992) Comparison of the outer and inner epidermis: inhibition of auxin-induced elongation of maize coleoptiles by glucan antibodies. Plant Physiol **98:** 1298–1303

**Huber DJ, Nevins DJ** (1981) Partial purification of endo- and exo-β-D-glucanase enzymes from *Zea mays* L. seedlings and their involvement in cell wall autohydrolysis. Physiol Plant **53:** 533–539

**Inouhe M, Nevins DJ** (1998) Changes in the activities and polypeptide levels of exo- and endo-glucanases in cell walls during developmental growth of *Zea mays* coleoptiles. Plant Cell Physiol **39:** 762–768

**Kacuráková M, Capek P, Sasinková V, Wellner N, Ebringerová A** (2000) FT-IR study of plant cell wall model compounds: pectic polysaccharides and hemicelluloses. Carbohydr Polym **43:** 195–203

**Kato Y, Nevins DJ** (1984) Enzymic dissociation of *Zea* shoot cell wall polysaccharides. II. Dissociation of (1→3),(1→4) β-D-glucan by purified (1→3),(1→4) β-D-glucan 4-glucanohydrolase from *Bacillus subtilis*. Plant Physiol **75:** 745–752

**Kemsley EK** (1998) Discriminant Analysis of Spectroscopic Data. John Wiley and Sons, Chichester, UK

**Kim J-B, Carpita NC** (1992) Esterification of maize cell wall pectins related to cell expansion. Plant Physiol **98:** 646–653

**Kim J-B, Olek AT, Carpita NC** (2000) Plasma membrane and cell wall exo-β-D-glucanases in developing maize coleoptiles. Plant Physiol **123:** 471–485

**Kutschera U** (1989) Tissue stresses in growing plant organs. Physiol Plant **77:** 157–163

**Liang CY, Marchessault RH** (1959) Infrared spectra of crystalline polysaccharides: II. Native celluloses in the region from 640 to 1700 $cm^{-1}$. J Polym Sci **39:** 269–278

**McCann MC, Chen L, Roberts K, Kemsley EK, Séné C, Carpita NC, Stacey NJ, Wilson RH** (1997) Infrared microspectroscopy: sampling heterogeneity in plant cell wall composition and architecture. Physiol Plant **100:** 729–738

**McCann MC, Hammouri M, Wilson R, Belton P, Roberts K** (1992) Fourier transform infrared microspectroscopy is a new way to look at plant cell walls. Plant Physiol **100:** 1940–1947

**McCann MC, Roberts K** (1991) Architecture of the primary cell wall. *In* CW Lloyd, ed, The Cytoskeletal Basis of Plant Growth and Form. Academic Press, London, pp 109–129

**McCann MC, Wells B, Roberts K** (1990) Direct visualisation of cross-links in the primary plant cell wall. J Cell Sci **96:** 323–334

**Meikle PJ, Hoogenraad NJ, Bonig I, Clarke AE, Stone BA** (1994) A (1→3),(1→4) β-D-glucan-specific monoclonal antibody and its use in the quantitation and immunocytochemical location of (1→3),(1→4) β-D-glucans. Plant J **5:** 1–5

**Müsel G, Schindler T, Bergfeld R, Ruel K, Jacquet G, Lapierre C, Speth V, Schopfer P** (1997) Structure and distribution of lignin in primary and secondary cell walls of maize coleoptiles analyzed by chemical and immunological probes. Planta **201:** 146–159

**Pritchard J, Hetherington PR, Fry SC, Tomos AD** (1993) Xyloglucan endotransglycosylase activity, microfibril orientation and the profiles of cell wall properties along growing regions of maize roots. J Exp Bot **44:** 1281–1289

**Richmond PA** (1983) Patterns of cellulose microfibril deposition and rearrangement in Nitella: in vivo analysis by birefringence index. J Appl Polym Sci **37:** 107–122

**Scalbert A, Monties B, Lallemand J-Y, Guittet E, Rolando C** (1985) Ether linkage between phenolic acids and lignin fractions from wheat straw. Phytochemistry **24:** 1359–1362

**Séné CFB, McCann MC, Wilson RH, Grinter R** (1994) Fourier-transform Raman and Fourier-transform infrared spectroscopy - an investigation of 5 higher plant cell walls and their components. Plant Physiol **106:** 1623–163

**Sugimoto K, Williamson RE, Wasteneys GO** (2000) New techniques enable comparative analysis of microtubule orientation, wall texture and growth rate in intact roots of Arabidopsis. Plant Physiol **124:** 1493–1506

**Talbott LD, Ray PM** (1992) Molecular size and separability features of pea cell-wall polysaccharides: Implications for models of primary wall structure. Plant Physiol **98:** 357–368

**Titel C, Ehwald R** (1999) Permeability limits of cell walls in suspension cultures: biotechnological and physiological aspects. Russ J Plant Physiol **46:** 739–744

**Tsuboi M** (1957) Infrared spectrum and crystal structure of cellulose. J Polym Sci **25:** 159–171

**Updegraff D** (1969) Semimicro determination of cellulose in biological materials. Anal Biochem **32:** 420–424

**Wells B** (1985) Low temperature box and tissue handling device for embedding biological tissue for immunostaining in electron microscopy. Micron Microscp Acta **16:** 49–53

**Whitney SE, Gidley MJ, McQueen-Mason S** (2000) Probing expansin action using cellulose/hemicellulose composites. Plant J **22:** 327–334